arXiv:1406.3659v1 [physics.plasm-ph] 13 Jun 2014

Dynamical spin effects in ultra-relativistic laser pulses

Meng Wen,[1,*] Heiko Bauke,[1,†] and Christoph H. Keitel[1]

[1]Max-Planck-Institut für Kernphysik, Saupfercheckweg 1, 69117 Heidelberg, Germany

(Dated: June 17, 2014)

The dynamics of single laser-driven electrons and many particle systems with spin are investigated on the basis of a classical theory. We demonstrate that the spin forces can alter the electron dynamics in an ultra-relativistic laser field due to the coupling of the electron's spin degree of freedom to its kinematic momentum. High-energy electrons can acquire significant spin-dependent transverse momenta while passing through a counterpropagating ultra-relativistic infrared laser pulse. Numerical calculations show that the deflection of the electrons by the laser pulse is determined by the laser intensity, the pulse duration, and the initial spin orientation of the electron. We complement our investigation of these dynamical spin effects by performing particle-in-cell simulations and point out possibilities of an experimental realization of the predicted effect with available laser parameters.

PACS numbers: 41.75.Jv, 42.65.Sf, 52.27.Ny, 79.20.Ds

Introduction The spin was introduced as an intrinsic property of the electron in order to explain the emission spectra of alkali metals and the Stern-Gerlach experiment. Spin dynamics and spin effects were widely investigated, e. g., in semiconductors [1], diamond [2], graphene [3], quantum plasmas [4], gases [5], and also undulators [6]. It appears naturally in the framework of relativistic quantum mechanics governed by the Dirac equation. However, a classical description of the electron spin may be found phenomenologically or via a correspondence principle [7, 8]. The classical theory of spin was first laid down by Frenkel [9] and Thomas [10, 11] and further developed by Bargmann, Michel, and Telegdi (BMT) [12] and others. It is commonly used to study the spin precession, e. g., in gravitation [13], in ferromagnetic crystals [14, 15], and in high-energy physics [16, 17].

The investigation of spin effects has become relevant in particular due to recent developments in particle accelerators and the availability of high-intensity lasers [18]. Electron sources that utilize laser-driven acceleration provide electron bunches with the size of a few micrometers [19], a divergence of a few milliradians [20], an energy of hundreds of megaelectronvolts and an energy spread of 1 % [21]. Laser intensities have reached the ultra-relativistic domain at $10^{22}\,\mathrm{W/cm^2}$ [22] and push research in laser-matter interaction into the quantum electrodynamics domain [23, 24]. Predicted phenomena such as non-dipole effects [25], radiation reaction [26–30], vacuum-polarization effects [31], and pair production [32] may be realized experimentally. In particular, spin effects are expected to occur at ultra-high intensities [33–39]. Angular-momentum related properties of electron bunches, such as vortices in plasmas [40], beam angular-momentum [41], and spin polarization [42, 43] have been studied. To describe spin effects of energetic particles in fields [44–46] and especially in the complex environment of plasmas we have to rely on classical physics. This can be accomplished by considering additional terms in the classical equation of motion of charged particles, as it is realized for QED effects in the Landau-Lifshitz equation [47–50].

In this letter we study spin dynamics of free electrons classically in ultra-relativistic laser fields. We demonstrate that the coupling between spin and kinematic momentum can modify the electron's spatial motion significantly for feasible relativistic parameters as compared to spinless particles.

Equations of motion for electrons with spin In classical theories, the spin of an electron with rest mass m and charge $q = -e$ is characterized by a unit vector $\boldsymbol{s}$, corresponding to the direction of the spin's quantum mechanical expectation value. The magnetic moment $\boldsymbol{\mu}$ of an electron is proportional to the spin vector $\boldsymbol{\mu} = g\mu_\mathrm{B}\boldsymbol{s}/2$, with the gyromagnetic factor $g \approx 2$, the Bohr magneton $\mu_\mathrm{B} = q\hbar/(2mc)$ and c and $\hbar$ denoting the speed of light and the reduced Planck constant, respectively. Following Frenkel [9], it is convenient to incorporate the spin dynamics into the electron's equations of motion by introducing the spin tensor $\Pi_{\alpha\beta}$, which is defied as [51]

$$\Pi_{\alpha\beta} = \begin{pmatrix} 0 & -T_x & -T_y & -T_z \\ T_x & 0 & -\Pi_z & \Pi_y \\ T_y & \Pi_z & 0 & -\Pi_x \\ T_z & -\Pi_y & \Pi_x & 0 \end{pmatrix} =: (\boldsymbol{T}, \boldsymbol{\Pi}), \tag{1}$$

with $\boldsymbol{T}$ denoting the electric moment $\boldsymbol{T} = \gamma\boldsymbol{\beta} \times \boldsymbol{s}$ and $\boldsymbol{\Pi}$ the magnetic moment $\boldsymbol{\Pi} = \gamma\boldsymbol{s} - \gamma^2(\boldsymbol{\beta}\cdot\boldsymbol{s})\boldsymbol{\beta}/(\gamma+1)$. Here γ is the Lorentz factor and $\boldsymbol{\beta} = \boldsymbol{v}/c$ the normalized velocity of the electron. Then the spin potential energy is induced by the electron's magnetic moment $-\boldsymbol{\mu}\cdot\boldsymbol{B}' = -g\mu_\mathrm{B}\Pi_{\alpha\beta}F^{\alpha\beta}/4$, in which $\boldsymbol{B}' = \gamma(\boldsymbol{B} + \boldsymbol{E}\times\boldsymbol{\beta}) - \gamma^2\boldsymbol{\beta}(\boldsymbol{\beta}\cdot\boldsymbol{B})/(\gamma+1)$ represents the magnetic field in the electron's rest frame and $F^{\alpha\beta} = \partial^\alpha A^\beta - \partial^\beta A^\alpha =: (\boldsymbol{E}, \boldsymbol{B})$ indicates the four-tensor of the electromagnetic, the corresponding four-vector potential A^α, and the electric $\boldsymbol{E}$ and magnetic $\boldsymbol{B}$ fields in the laboratory frame [52]. Requiring $\gamma\mathcal{L}$ to be Lorentz invariant [53], the Lagrangian function $\mathcal{L}$ of the relativistic particle is given by [54]

$$\mathcal{L} = -\frac{mc^2}{\gamma} + \frac{g\mu_B}{4\gamma}\Pi_{\alpha\beta}F^{\alpha\beta} - \frac{q}{c}v_\alpha A^\alpha, \tag{2}$$

where $v_\alpha = (c, -\boldsymbol{v})$ is the four-velocity of the particle and $qv_\alpha A^\alpha/c$ equals the electromagnetic potential energy. The electron's equations of motion for the position $\boldsymbol{r}$ and the momentum

$\boldsymbol{p} = m\gamma\boldsymbol{v}$ follow from the Lagrangian (2) via the Euler-Lagrange equations as

$$\eta\frac{\mathrm{d}}{\mathrm{d}t}\boldsymbol{p} = q(\boldsymbol{E} + \boldsymbol{\beta}\times\boldsymbol{B}) + \boldsymbol{f}_S\,, \tag{3a}$$

$$\frac{\mathrm{d}}{\mathrm{d}t}\boldsymbol{r} = \frac{\boldsymbol{p}}{m\gamma}\,, \tag{3b}$$

with

$$\boldsymbol{f}_S = \frac{g}{2}\gamma\mu_\mathrm{B}\left(\frac{\boldsymbol{\nabla}}{\gamma^2} + \boldsymbol{\beta}\frac{\mathrm{d}}{c\mathrm{d}t}\right)(\boldsymbol{s}\cdot\boldsymbol{B}')\,, \tag{3c}$$

$$\eta = 1 - \frac{g}{2}\frac{\mu_\mathrm{B}}{mc^2}\boldsymbol{s}\cdot\boldsymbol{B}'\,, \tag{3d}$$

in agreement with Ref. [54]. The force in (3a) acting on the electron is given by the well-known Lorentz force plus the spin force $\boldsymbol{f}_S$ that both are modified by the spin potential related factor η. Note that $\mathrm{d}\boldsymbol{B}'/\mathrm{d}t$ can also be written as $-\boldsymbol{\nabla}\times\boldsymbol{E}' + (c\boldsymbol{\beta}\cdot\boldsymbol{\nabla})\boldsymbol{B}'$ by introducing the electric field $\boldsymbol{E}'$ in the electron's rest frame that is related to $\boldsymbol{B}'$ via the Maxwell-Faraday equation. Thus, the spin force (3c) originates from the inhomogeneities of electromagnetic fields. Furthermore, the electron's momentum couples to the spin that precesses in the electromagnetic fields under the effect of the BMT equations [12]. Taking into account the electron's equation of motion (3) the BMT equations are given by

$$\frac{\mathrm{d}\boldsymbol{s}}{\mathrm{d}t} = \boldsymbol{\Omega}_0 + \boldsymbol{\Omega}_1\,, \tag{4a}$$

$$\boldsymbol{\Omega}_0 = \frac{q}{mc}\boldsymbol{s}\times\left[\eta_1\boldsymbol{B} - \eta_2\boldsymbol{E}\times\boldsymbol{\beta} - \eta_3\frac{\gamma}{\gamma+1}\boldsymbol{\beta}\,(\boldsymbol{\beta}\cdot\boldsymbol{B})\right], \tag{4b}$$

$$\boldsymbol{\Omega}_1 = \frac{g}{2}\frac{\mu_\mathrm{B}}{\eta mc}\frac{1}{\gamma+1}\boldsymbol{s}\times(\boldsymbol{\beta}\times\boldsymbol{\nabla})\,(\boldsymbol{s}\cdot\boldsymbol{B}')\,, \tag{4c}$$

where $\boldsymbol{\Omega}_0$ is the contribution to the spin precession by the electromagnetic fields in zeroth order with $\eta_1 = g/2-(\gamma-1)/(\gamma\eta)$, $\eta_2 = g/2-\gamma/\eta/(\gamma+1)$, and $\eta_3 = g/2-1/\eta$; while $\boldsymbol{\Omega}_1$ accounts for field gradients [55].

Radiation reaction may cause additional damping forces that may be incorporated into (3a) via the additional force term $\boldsymbol{f}_R$, which is part of the four-vector $f_R^\alpha = (f_R^0, \boldsymbol{f}_R) = r_e(q\gamma\partial_\gamma F^{\alpha\beta}v_\beta v^\gamma + q^2F^{\alpha\beta}F_{\beta\gamma}v^\gamma/mc - q^2\gamma^2F^{\beta\gamma}F_{\gamma\delta}v^\delta v_\beta v^\alpha/mc^3)$ with $r_e \approx 1.18\times10^{-8}$ µm [56]. In all calculations of this work we take into account the effects of radiation damping by adding $\boldsymbol{f}_R$ on the right hand side of (3a). Modifications of the BMT equations (4) due to radiation damping are found negligible for the parameters employed here.

Electrons counterpropagating laser fields We consider a plane wave with circular polarization propagating along the x axis with its vector potential $\boldsymbol{A} = \boldsymbol{a}mc^2/e$, and electric and magnetic fields $\boldsymbol{E} = -\partial_t\boldsymbol{A}/c$ and $\boldsymbol{B} = \boldsymbol{\nabla}\times\boldsymbol{A}$, where the scaled vector potential $\boldsymbol{a} = (0, a_y, a_z)$ with $a_y + ia_z = a_0\sin^2(\pi\tau/T)\exp(i\omega_L\tau)$ and the scaled field's amplitude $a_0 = (I_0/\pi)^{1/2}e\lambda_L/(mc^{5/2})$ depends on the laser intensity I_0, the phase $\omega_L\tau = \omega_L(t-x/c)$, the duration T of the laser pulse, and the angular frequency $\omega_L = 2\pi/\tau_L = 2\pi c/\lambda_L$ with the laser's wavelength λ_L and its period τ_L. In the case of interest here with $\gamma_0 \gg 1$, the $\boldsymbol{\nabla}/\gamma^2$ term in (3c) can be neglected, where γ_0 is the Lorentz factor at time $t = 0$. Then the dominant term of the spin force originates from the total time derivative of the magnetic field, which includes a partial time derivative and spatial gradients $\mathrm{d}\boldsymbol{B}'/\mathrm{d}t = (\partial/\partial t + c\boldsymbol{\beta}\cdot\boldsymbol{\nabla})\boldsymbol{B}'$.

The magnitude of the spin force can be estimated from the dominant term of Eq. (3c), i. e., $\boldsymbol{f}_S \approx g\mu_\mathrm{B}\boldsymbol{p}/(2mc^2)\,\mathrm{d}(\boldsymbol{s}\cdot\boldsymbol{B}')/\mathrm{d}t$, which depends on the particle's momentum $\boldsymbol{p}$ as well as on the spin vector $\boldsymbol{s}$ and $\boldsymbol{B}'$. The momentum of an energetic electron counterpropagating in a plane wave with $\gamma_0 > a_0$ remains in the longitudinal direction $p_x \approx -\gamma mc$ and the electromagnetic fields cause $\boldsymbol{p}_\perp \approx \boldsymbol{a}mc$. Thus, the velocity $\boldsymbol{\beta}$ is almost perpendicular to $\boldsymbol{B}$ and therefore $\boldsymbol{B}' \approx 2\gamma\boldsymbol{B}$. Furthermore, the spin vector $\boldsymbol{s}$ oscillates in the laser field but remains close to its initial value, especially for relatively low laser intensities. This is demonstrated in Fig. 1(a), which shows the y component of the spin vector for an electron with initial spin direction $\boldsymbol{s} = \boldsymbol{e}_y$. Thus, with $\boldsymbol{s} \approx \boldsymbol{e}_y$ and $\boldsymbol{B}' \approx 2\gamma\boldsymbol{B}$, we get $\mathrm{d}(\boldsymbol{s}\cdot\boldsymbol{B}')/\mathrm{d}t \approx 2\gamma(1-\beta_x)a_z m\omega_L^2 c/e$ and the counterpropagating setup, where $(1-\beta_x) \approx 2$, maximizes the spin force. Finally, the dominant term of the spin force can be expressed by the laser field $\boldsymbol{a}$ and the electron's energy γ as $\boldsymbol{f}_S \approx (-\gamma, a_y, a_z)\,a_z\gamma g m\omega_L c\lambda_e/\lambda_L$ with the Compton wavelength $\lambda_e = 4\pi\mu_\mathrm{B}/q$ ($\lambda_e/\lambda_L = 3.03\times10^{-6}$ for a laser wavelength of $\lambda_L = 800$ nm). Thus, $\boldsymbol{f}_S$ increases with rising laser intensity and initial electron energy. For relativistic particles in strong fields it may become even comparable to the Lorentz force. The relative weight of the spin force $\boldsymbol{f}_S$ in (3a) reaches around 6 % of the amplitude of the Lorentz force for $a_0 \sim \gamma_0 \sim 10^2$.

When a spinless particle passes through a time-symmetric laser pulse, its transverse momentum does not increase due to the symmetric oscillations of the directions of the Lorentz force [57] and the radiation reaction force [58]. This symmetry is broken by the spin force $\boldsymbol{f}_S$ if the particle features a spin degree of freedom, e. g., for electrons. The spin force $\boldsymbol{f}_S$ oscillates in the laser field, see Figs. 1(b) and (c). The x component of the spin force $f_{Sx} \propto \gamma^2 a_z$ oscillates synchronously with the magnetic field and its effect averages out over several laser cycles, see Fig. 1(b). Similarly, the y component also oscillates symmetrically $f_{Sy} \propto \gamma a_y a_z$ with vanishing net effect. However, the z component of the spin force, which is in leading order $f_{Sz} \propto \gamma a_z^2$, varies with the frequency $2\omega_L$ and remains positive for all times, see Fig. 1(c). Consequently, a spin-force effect is accumulated to a significant extra momentum over the duration of the laser pulse. Note that the contribution of laser fields to f_{Sz} arise only via a_z. Thus, a linearly polarized pulse $\boldsymbol{a} = (0, 0, a_z)$ counterpropagating to an electron with initial spin $\boldsymbol{s} = \boldsymbol{e}_y$ would yield similar effects as circularly polarized pulses.

The effect of the spin forces becomes explicit by comparing the time-evolution of the momentum of spinless particles with that of electrons as shown in Fig. 2. Initially, the particles move along the x coordinate to the left such that they encounter the laser pulse at $t = 0$ and $x = 0$. The equation of motion for spinless particles involves the Lorentz force and radiation reaction yielding the solid (red) curves in Fig. 2. In this case, the

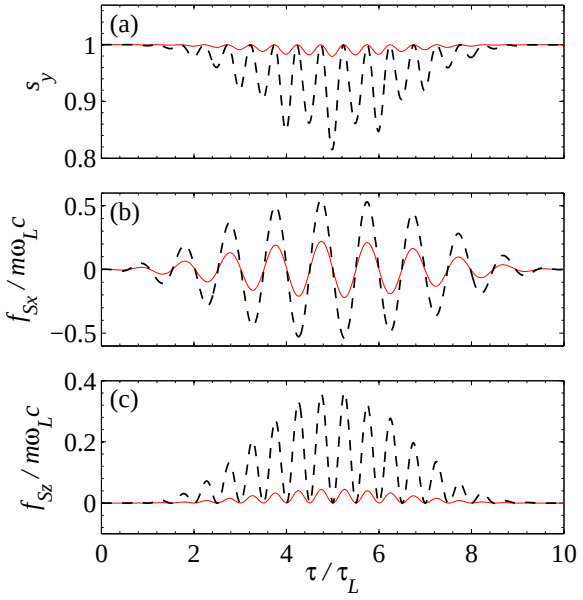

FIG. 1: (color online) (a) The y component of the spin vector as it evolves under Eq. (4) as a function of $\tau = t - x(t)/c$. (b), (c) The evolution of the x and z components of the spin force $\boldsymbol{f}_S$ for two different peak intensities. Solid (red) and dashed (black) curves correspond to an intensity of $I_0 = 4.28 \times 10^{20}\,\mathrm{W/cm^2}$ ($a_0 = 10$) and $I_0 = 3.85 \times 10^{21}\,\mathrm{W/cm^2}$ ($a_0 = 30$), respectively. The laser's wavelength equals $\lambda_L = 800\,\mathrm{nm}$ and the pulse duration is $T = 10\tau_L$ with $\tau_L = \lambda_L/c$. The electron's initial energy corresponds to $\gamma_0 = 50$.

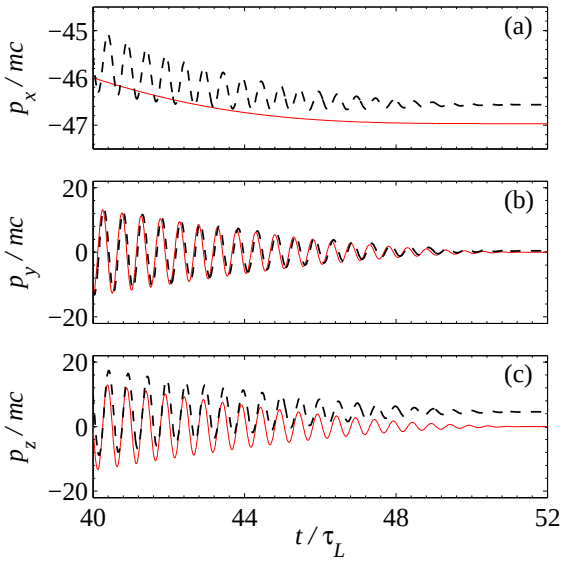

FIG. 2: (color online) Evolution of the momenta p_x (a), p_y (b) and p_z (c) at the end of the interaction with the laser pulse for particles with initially $\gamma_0 = 50$. Solid (red) and dashed (black) curves correspond to spinless particles and electrons with spin, respectively. The laser intensity is the same as in Fig. 1(b), with the duration $T = 100\tau_L$.

transverse momenta vary symmetrically over the interaction time. As a net effect of radiation reaction the final longitudinal momentum $|p_x| = 47$ is smaller than the initial $|p_{x0}| = 50$. The dynamics changes, however, when the spin is taken into account via the coupled Eqs. (3) and (4). The momentum evolution of an electron in an ultra-relativistic laser pulse and with initial spin $\boldsymbol{s} = \boldsymbol{e}_y$ is indicated by the dashed (black) curves in Fig. 2. As a consequence of the spin force, the transverse momentum components after interaction with the laser pulse differ from the initial momenta. Thus, the interaction of the electron with the laser field has a non-vanishing net effect on the electron's transverse momenta. Furthermore, the damping of the longitudinal momentum is stronger as compared to spinless particles via extra acceleration from the spin force, see solid (red) and dashed (black) lines in Fig. 2. For the parameters in Fig. 2, for example, the electron's initial momentum is $(-50, 0, 0)mc$ but its final value yields $(-46.56, 0.44, 4.62)mc$. Further numerical calculations indicate that if a focused laser pulse is considered [59] the spin effect does not change qualitatively as compared to the plane wave case as long as the focus waist is larger than several laser wavelengths.

Experimentally the momentum transfer in the laser field may be verified via the determination of the deflection $p_\perp/|p_x|$ with $p_\perp = (p_y^2 + p_z^2)^{1/2}$ instead of measuring the individual momentum components. For an unpolarized electron beam the deflection will happen symmetrically around the laser's propagation axis. Figure 3 presents how the deflection of an electron that is initially polarized along the y direction depends on the laser's amplitude a_0 and the pulse duration T. The deflection does not depend on γ_0 directly. However, γ_0 has to be at least larger than $a_0/2$ to maintain the counterpropagating regime. The deflection becomes larger for higher laser intensities and also growths with the pulse duration T, see Fig. 3. For the employed field strengths a_0 and pulse durations T, the deflection $p_\perp/|p_x|$ depends quadratically on the field strength and linearly on the pulse duration. It can be estimated as $p_\perp/|p_x| \approx (1/2)(\lambda_e/\lambda_L)a_0^2(T/\tau_L)$.

Particle-in-cell simulations In order to investigate how the dynamical spin effect changes the dynamics for a whole bunch of electrons we performed particle-in-cell (PIC) simulations [60] employing a 1D3V-model which is one-dimensional in position and three-dimensional in velocity space. The reduction to one dimension in position space is justified because the electromagnetic field of the laser depends on the x coordinate only when laser focusing is negligible. The PIC simulations include the spin degree of freedom as an additional property of the pseudo particles as well as radiation reaction. In each time step the coupled equations of motion Eqs. (3) and (4) are integrated for all pseudo particles. To simulate spin precession, a Boris' rotation [61, 62] of the spin is performed while its momentum rotates between the two stages of half-accelerations in each time step. The field gradients are calculated via linear interpolation of the fields at adjacent cell boundaries.

Figure 4 shows the transverse momentum distribution of a particle bunch after interaction with a counterpropagating circularly polarized laser pulse for (a) spinless particles, (b)

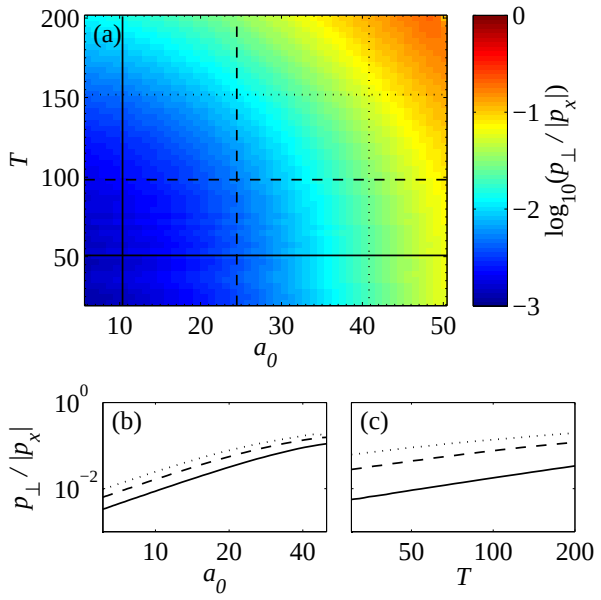

FIG. 3: (color online) (a) The dependencies of the final deflection $p_\perp/|p_x|$ for an electron with initial spin $\boldsymbol{s} = \boldsymbol{e}_y$ on the laser field's amplitude a_0 and on the duration T. The solid, dashed, and dotted curves in (b) and (c) correspond to the horizontal and vertical curves in (a). The color in (a) refers to the logarithm of $p_\perp/|p_x|$. The initial electron energy corresponds to $\gamma_0 = 50$. The quantum parameter $\chi_0 = 4.4\times10^{-6}\gamma_0 a_0$ [24] is $1.1\times10^{-3} < \chi_0 < 1.1\times10^{-2}$ for the cases $5 < a_0 < 50$ investigated here.

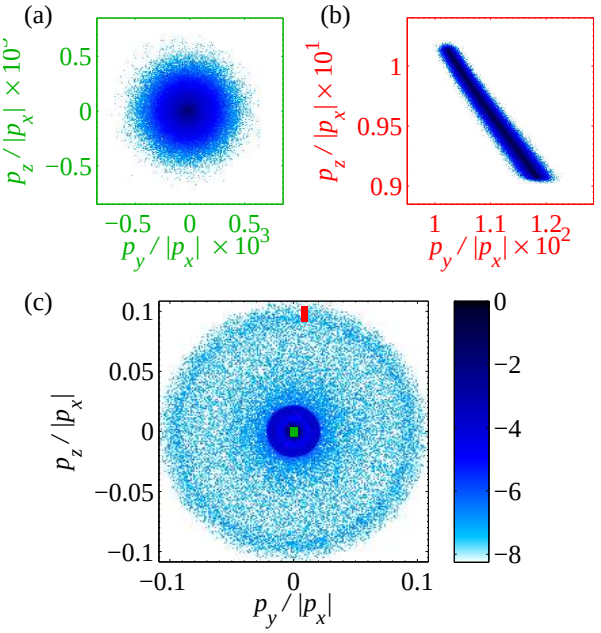

FIG. 4: (color online) PIC simulated transverse momentum distribution of a particle bunch after interaction with a counterpropagating circularly polarized laser pulse for spinless particles (a), for initially y polarized electrons (b), and for initially unpolarized electrons (c). The color indicates the logarithm of the distribution's density in arbitrary units. Note the different scales of the various subfigures. The green and red rectangles in subfigure (c) indicate the regions of the momentum spaces that are shown in subfigures (a) and (b). The laser pulse has an intensity of $I_0 = 3.85\times10^{21}\,\mathrm{W/cm^2}$ ($a_0 = 30$) and consists of 100 cycles. Initially the bunch is directed strictly along the x direction with an energy of each electron $\gamma_0 = 50$ and a divergence of 1 mrad. The initial bunch has a length of $l_e = 5\lambda_L = 4\,\mu\mathrm{m}$ and a density of $n_e = 0.001 n_c \approx 1.7\times10^{18}\,\mathrm{cm^{-3}}$, where $n_c = \pi mc^2/(\lambda_L e)^2$ refers to the critical plasma density.

initially y polarized electrons, and (c) initially unpolarized electrons. For the spinless case shown in Fig. 4(a) the divergence of the bunch changes marginally during its interaction with the laser pulse. The electron-bunch's expansion by the Coulomb potential is very weak due to the electrons' high energy and the low density. If the spin of the particles is taken into account, however, electrons of a fully polarized bunch are deflected by the spin forces, see Fig. 4(b). This effect appears detectable experimentally. The amount of the bunch's deflection agrees with the prediction for the singe-electron case considered in Fig. 3. An unpolarized electron bunch with the initial spin orientation distributed homogeneously in all directions is considered in Fig. 4(c). The final momentum distribution is symmetric around the laser's propagation direction and most electrons are deflected by an angle that is predicted by singe-electron trajectories. Thus, a significant increase of the divergence angle to $\theta = 2\arctan(p_\perp/|p_x|) \approx 198$ mrad results.

Discussion and conclusion We investigated electron motion in strong laser fields focussing on spin effects. For this purpose we applied classical equations of motion for the electron's position, kinematic momentum, and its spin. These coupled equations were derived from a Lorentz invariant Lagrangian and are a generalization of the well-known BMT equations. We apply this theory to the interaction of an electron bunch with a counterpropagating high-intensity laser pulse. In this setting, electrons are deflected significantly by the spin force, which originates from the particles' high energy, strong laser gradients as well as the spin component along the magnetic field. Focusing and polarization states of the laser pulse do not change this effect qualitatively. These results were obtained by solving numerically the equations of motion for single electrons and further confirmed by PIC simulations for an electron bunch with parameters suitable for a possible experimental realization of this effect. In conclusion, the influence of the spin on the motion of an electron should be taken into account in the indicated situations of light-matter interaction at relativistic intensities with strong laser inhomogeneities, long interaction time and highly preaccelerated particles.

We would like to thank Dr. A. Di Piazza and Dr. K. Z. Hatsagortsyan for valuable discussions.

* meng.wen@mpi-hd.mpg.de
† heiko.bauke@mpi-hd.mpg.de

[1] T. Li, A. Patz, L. Mouchliadis, J. Yan, T. A. Lograsso, I. E. Perakis, and J. Wang, Nature **496**, 69 (2013).
[2] M. S. Blok, M. L. Bonato, C. Markham, D. J. Twitchen, V. V. Dobrovitski, and R. Hanson, Nat. Phys. **10**, 189 (2014).
[3] J. Güttinger, T. Frey, C. Stampfer, T. Ihn, and K. Ensslin, Phys. Rev. Lett. **105**, 116801 (2010).
[4] M. Marklund and G. Brodin, Phys. Rev. Lett. **98**, 025001 (2007).
[5] M. C. Beeler, R. A. Williams, K. Jiménez-García, L. J. LeBlanc, A. R. Perry, and I. B. Spielman, Nature **498**, 201 (2013).
[6] S. Mane, Nucl. Instrum. Methods Phys. Res., Sect. A **675**, 15 (2012).
[7] A. J. Silenko, Phys. Rev. A **77**, 012116 (2008).
[8] M. W. Walser, C. Szymanowski, and C. H. Keitel, Europhysics Letters **48**, 533 (1999).
[9] J. Frenkel, Z. Phys. **37**, 243 (1926).
[10] L. H. Thomas, Nature **117**, 514 (1926).
[11] L. H. Thomas, Philosophical Magazine Series 7 **3**, 1 (1927).
[12] V. Bargmann, V. L. Telegdi, and L. Michel, Phys. Rev. Lett. **2**, 435 (1959).
[13] B. Mashhoon and Y. N. Obukhov, Phys. Rev. D **88**, 064037 (2013).
[14] D. Landau and E. Lifshitz, Phys. Z. Sowjetunion **8**, 153 (1935).
[15] R. Wieser, Phys. Rev. Lett. **110**, 147201 (2013).
[16] S. R. Mane, Y. M. Shatunov, and K. Yokoya, Rep. Prog. Phys. **68**, 1997 (2005).
[17] J. Vieira, C.-K. Huang, W. B. Mori, and L. O. Silva, Phys. Rev. ST Accel. Beams **14**, 071303 (2011).
[18] G. Mourou, T. Tajima, and S. Bulanov, Rev. Mod. Phys. **78**, 309 (2006).
[19] O. Lundh, J. Lim, C. Rechatin, L. Ammoura, A. Ben-Ismail, X. Davoine, G. Gallot, J.-P. Goddet, E. Lefebvre, V. Malka, and J. Faure, Nat. Phys. **7**, 219 (2011).
[20] G. R. Plateau, C. G. R. Geddes, D. B. Thorn, M. Chen, C. Benedetti, E. Esarey, A. J. Gonsalves, N. H. Matlis, K. Nakamura, C. B. Schroeder, S. Shiraishi, T. Sokollik, J. van Tilborg, C. Toth, S. Trotsenko, T. S. Kim, M. Battaglia, T. Stöhlker, and W. P. Leemans, Phys. Rev. Lett. **109**, 064802 (2012).
[21] C. Rechatin, J. Faure, A. Ben-Ismail, J. Lim, R. Fitour, A. Specka, H. Videau, A. Tafzi, F. Burgy, and V. Malka, Phys. Rev. Lett. **102**, 164801 (2009).
[22] V. Yanovsky, V. Chvykov, G. Kalinchenko, P. Rousseau, T. Planchon, T. Matsuoka, A. Maksimchuk, J. Nees, G. Cheriaux, G. Mourou, and et al., Opt. Express **16**, 2109 (2008).
[23] G. A. Mourou, C. L. Labaune, M. Dunne, N. Naumova, and V. T. Tikhonchuk, Plasma Physics and Controlled Fusion **49**, B667 (2007).
[24] A. Di Piazza, C. Müller, K. Z. Hatsagortsyan, and C. H. Keitel, Rev. Mod. Phys. **84**, 1177 (2012).
[25] M. Klaiber, E. Yakaboylu, H. Bauke, K. Z. Hatsagortsyan, and C. H. Keitel, Phys. Rev. Lett. **110**, 153004 (2013).
[26] A. Di Piazza, K. Z. Hatsagortsyan, and C. H. Keitel, Phys. Rev. Lett. **102**, 254802 (2009).
[27] Y. Hadad, L. Labun, J. Rafelski, N. Elkina, C. Klier, and H. Ruhl, Phys. Rev. D **82**, 096012 (2010).
[28] C. Harvey, T. Heinzl, and M. Marklund, Phys. Rev. D **84**, 116005 (2011).
[29] L. L. Ji, A. Pukhov, I. Y. Kostyukov, B. F. Shen, and K. Akli, Phys. Rev. Lett. **112**, 145003 (2014).
[30] D. G. Green and C. N. Harvey, Phys. Rev. Lett. **112**, 164801 (2014).
[31] A. Di Piazza, K. Z. Hatsagortsyan, and C. H. Keitel, Phys. Rev. Lett. **100**, 010403 (2008).
[32] J. Schwinger, Phys. Rev. **82**, 664 (1951).
[33] M. W. Walser, D. J. Urbach, K. Z. Hatsagortsyan, S. X. Hu, and C. H. Keitel, Phys. Rev. A **65**, 043410 (2002).
[34] F. H. M. Faisal and S. Bhattacharyya, Phys. Rev. Lett. **93**, 053002 (2004).
[35] G. Brodin, M. Marklund, J. Zamanian, and M. Stefan, Plasma Phys. Controlled Fusion **53**, 074013 (2011).
[36] S. Ahrens, H. Bauke, C. H. Keitel, and C. Müller, Phys. Rev. Lett. **109**, 043601 (2012).
[37] M. Boca, V. Dinu, and V. Florescu, Nucl. Instrum. Methods Phys. Res., Sect. B **279**, 12 (2012).
[38] T.-O. Müller and C. Müller, Phys. Rev. A **86**, 022109 (2012).
[39] M. Klaiber, E. Yakaboylu, C. Müller, H. Bauke, G. G. Paulus, and K. Z. Hatsagortsyan, J. Phys. B: At., Mol. Opt. Phys. **47**, 065603 (2014).
[40] M. Schwabe, S. Zhdanov, C. Räth, D. B. Graves, H. M. Thomas, and G. E. Morfill, Phys. Rev. Lett. **112**, 115002 (2014).
[41] C. Thaury, E. Guillaume, S. Corde, R. Lehe, M. Le Bouteiller, K. Ta Phuoc, X. Davoine, J. M. Rax, A. Rousse, and V. Malka, Phys. Rev. Lett. **111**, 135002 (2013).
[42] N. Raab, M. Büscher, M. Cerchez, R. Engels, l. Engin, P. Gibbon, P. Greven, A. Holler, A. Karmakar, A. Lehrach, R. Maier, M. Swantusch, M. Toncian, T. Toncian, and O. Willi, Physics of Plasmas (1994-present) **21**, 023104 (2014).
[43] K. Aulenbacher, The European Physical Journal Special Topics **198**, 361 (2011).
[44] Z. Huang and K.-J. Kim, Phys. Rev. ST Accel. Beams **10**, 034801 (2007).
[45] E. Esarey, C. B. Schroeder, and W. P. Leemans, Rev. Mod. Phys. **81**, 1229 (2009).
[46] S. Corde, K. Ta Phuoc, G. Lambert, R. Fitour, V. Malka, A. Rousse, A. Beck, and E. Lefebvre, Rev. Mod. Phys. **85**, 1 (2013).
[47] L. D. Landau and E. M. Lifshitz, *The Classical Theory of Fields*, 4th ed. (Butterworth-Heinemann, 1980).
[48] M. Tamburini, F. Pegoraro, A. Di Piazza, C. H. Keitel, T. Liseykina, and A. Macchi, Nuclear Instruments and Methods in Physics Research Section A: Accelerators, Spectrometers, Detectors and Associated Equipment **653**, 181 (2011).
[49] S. V. Bulanov, T. Z. Esirkepov, M. Kando, J. K. Koga, and S. S. Bulanov, Phys. Rev. E **84**, 056605 (2011).
[50] M. Tamburini, C. H. Keitel, and A. Di Piazza, Phys. Rev. E **89**, 021201 (2014).
[51] V. Bagrov and V. Bordovitsyn, Soviet Physics Journal **23**, 128 (1980).
[52] J. D. Jackson, *Classical Electrodynamics*, 3rd ed. (John Wiley & Sons, New York, 1998).
[53] M. W. Walser and C. H. Keitel, Letters in Mathematical Physics **55**, 63 (2001).
[54] A. O. Barut, *Electrodynamics and Classical Theory of Fields & Particles* (Dover Publications, New York, 1980).
[55] R. H. Good, Phys. Rev. **125**, 2112 (1962).
[56] C. Teitelboim, D. Villarroel, and C. van Weert, La Rivista del Nuovo Cimento **3**, 1 (1980).
[57] J. D. Lawson, IEEE Trans. Nucl. Sci. **26**, 4217 (1979).
[58] A. Di Piazza, Letters in Mathematical Physics **83**, 305 (2008).
[59] Y. I. Salamin and C. H. Keitel, Phys. Rev. Lett. **88**, 095005 (2002).
[60] H.-C. Wu, "JPIC & How to make a PIC code," (2011), arXiv:1104.3163.
[61] J. P. Boris, in *Proceedings of the conference on the numerical simulation of plasmas*, edited by J. P. Boris and R. A. Shanny (Naval Research Laboratory, Washington, D. C., 1970) pp. 3–67.
[62] C. K. Birdsall and A. B. Langdon, *Plasma physics via computer simulation* (Taylor and Francis, New York, 2005).